ResearchGate

See discussions, stats, and author profiles for this publication at: https://www.researchgate.net/publication/226609668

Design and In-line Raman Spectroscopic Monitoring of a Protein Batch Crystallization Process

ARTICLE *in* JOURNAL OF PHARMACEUTICAL INNOVATION · DECEMBER 2008

Impact Factor: 1 · DOI: 10.1007/s12247-008-9046-y

CITATIONS
3

READS
70

5 AUTHORS, INCLUDING:

Krizia M. Karry
Bristol-Myers Squibb
11 PUBLICATIONS **14** CITATIONS
SEE PROFILE

Rodolfo J Romañach
University of Puerto Rico at Mayagüez
45 PUBLICATIONS **395** CITATIONS
SEE PROFILE

Available from: Krizia M. Karry
Retrieved on: 26 January 2016

J Pharm Innov (2008) 3:271–279
DOI 10.1007/s12247-008-9046-y

RESEARCH ARTICLE

Design and In-line Raman Spectroscopic Monitoring of a Protein Batch Crystallization Process

Joanna Mercado · Manel Alcalà · Krizia M. Karry · Jorge L. Ríos-Steiner · Rodolfo J. Romañach

Published online: 14 November 2008
© International Society for Pharmaceutical Engineering 2008

Abstract Raman spectroscopy was used to design and monitor a lysozyme protein batch crystallization process in a lab scale study to facilitate the design of a pharmaceutical protein manufacturing process. A D-optimal design that consisted of 18 experiments was performed to elucidate the effect of temperature, concentration of the precipitating agent, time of crystallization, and possible interactions between these three factors on the Raman scattering changes. A polynomial mathematical model was calculated relating the scattering of the lysozyme solutions measured at individual Raman shifts to the significant factors obtained in the previous crystallization experiment. The 2,940-cm^{-1} band provided the highest correlation values indicative of small prediction errors and good predictive ability for the crystallization model. Raman scattering signals obtained during the experiments were used as input to obtain a response surface for the factors studied and elucidate the relationship between the crystallization process conditions and the crystals obtained. The main factors affecting the crystallization process were the sodium chloride concentration and temperature.

Keywords Raman spectroscopy · Crystallization · In-line monitoring · Process analytical technology · Quality by design

J. Mercado · M. Alcalà · K. M. Karry · J. L. Ríos-Steiner · R. J. Romañach (✉)
Department of Chemistry, University of Puerto Rico, Mayagüez Campus, P.O. Box 9019, Mayagüez 00681-9019, Puerto Rico
e-mail: rromanac@uprm.edu

Introduction

The current process analytical technology (PAT) initiative encourages the pharmaceutical industry to design manufacturing processes such that timely process measurements of critical quality parameters may be used to monitor and control such processes [1, 2]. The goals of this FDA initiative are to modernize and increase the efficiency of pharmaceutical manufacturing processes, and lower the risk of producing a poor quality product through a greater understanding of the manufacturing processes and raw materials used. This Food and Drug Administration (FDA) initiative started in 2002 and has triggered significant research efforts in industrial and academic laboratories to develop analytical methods to monitor pharmaceutical manufacturing processes [3]. Crystallization is one of the pharmaceutical processes that has received significant attention in the PAT initiative. NIR, mid-IR, and Raman spectroscopic methods are capable of providing in-line spectra without sample preparation, yielding important information for monitoring crystallization [4–7].

Raman spectroscopy provides flexibility for process measurements through its ability to collect spectra using both noninvasive and immersion probes. Furthermore, Raman spectra may be interpreted to obtain important structural information. The fact that water is a poor Raman scatterer makes Raman spectroscopy ideal to follow a number of reactions and crystallization processes in aqueous media. The main disadvantages are the low Raman cross-section and the low frequency noise associated with fluorescence arising from the analyte of interest or impurities. These disadvantages will usually not be significant in crystallization processes that are characterized by

the high concentrations needed for supersaturation and usually include previous purification steps that remove the principal process impurities. Taylor has already demonstrated the use of Raman spectroscopy to monitor the crystallization of flufenamic acid [5]. Berglund and coworkers showed that hanging drop crystallization may be monitored and controlled using Raman spectroscopy [8–12]. The methods developed by Berglund may be used to provide crystals of adequate particle size and purity to crystallographers interested in determining the crystal structure of a protein. Methods are also needed to facilitate the design of large-scale batch crystallization processes of FDA approved proteins and drugs. Furthermore, the pipelines of many pharmaceutical companies currently include increasing numbers of biotechnology-derived drug candidates.

This report describes a lab-scale study to aid in the design of a lysozyme protein batch crystallization process incorporating timely Raman measurements to monitor crystal growth. The Raman scattering signals, obtained as the concentration of the precipitating agent was varied over the temperature range of 15°C to 45°C, were used as input to obtain a response surface for the factors studied. The benefits of this approach also include a thorough understanding of the batch crystallization process as Raman scattering was used to elucidate the effect of temperature, concentration of the precipitating agent, time of crystallization, and possible interactions between these three factors. As indicated in ICH Q8: "Collection of process monitoring data during the development of the manufacturing process can provide useful information to enhance process understanding."[13]. The objectives of this study are not to investigate lysozyme crystallization, as it has been extensively studied [14–18], but to demonstrate an initial lab scale approach to enhance process understanding. The approach described may be used to design and facilitate protein crystallization for pharmaceutical manufacturing processes. This initial step in combination with additional efforts at larger scale could be used to implement PAT and quality by design protein crystallization processes.

Materials and Methods

Preparation of Lysozyme Solutions

Sodium acetate, Sigma Ultra, minimum 99.0%, acetic acid, Reagent Plus ≥99%, sodium Chloride Sigma Ultra, minimum 99.5% were purchased from Sigma Chemical Company (St. Louis, MO, USA). All solutions were prepared with deionized and double distilled water at room temperature. Three times crystallized, dialyzed, and lyophilized chicken egg white lysozyme was purchased from Sigma Chemical (catalog number L6876) and used without any further purification. Before use the lysozyme protein purity was first checked using a Centricon centrifugal filter device (Millipore, Billerica, MA, USA), where the maximum centrifugal force was 7,500×*g*. The lysozyme protein was dissolved into deionized water for an initial sample volume of 2.0 mL. The filtration process for the lysozyme protein was performed using an ultracel YM regenerated cellulose membrane with a nominal molecular weight limit of 3,000. The Raman spectra of the centrifuged and filtered lysozyme solutions was compared to that dissolved without prior treatment. The spectral comparison did not reveal any differences, and all further solutions were prepared without further purification.

A lysozyme stock solution (100 mg/mL) was prepared by dissolving the solid lysozyme protein into 0.1 M acetate buffer pH 4.5 and then filtered through a 0.22-μm Millipore filter before use. The acetate buffer was prepared by mixing equal amounts of acetic acid and sodium acetate and adjusting to pH 4.5 by adding either sodium hydroxide or hydrochloric acid. A Mettler Toledo digital meter was used to measure the pH of the acetate buffer. Aliquots from different lysozyme protein aqueous solution ranging from 0 to 90 mg/mL were prepared by dilution.

Raman Spectral Acquisition

Spectra were measured using a Raman Rxn1 System from Kaiser Optical Systems. (Ann Arbor, MI, USA) equipped with a 450-mW external cavity stabilized diode laser operating at 785 nm. The Raman spectrometer provides spectral coverage from 0 to 3,450 cm^{-1}. The spectrometer's intensity and wavelength calibration was performed before obtaining each set of spectra. The Holograms 4.0 software was used to acquire all spectra. Each spectrum was collected during 200 s using an exposure time of 10 s and five accumulations at 4 cm^{-1} resolution. A noncontact probe with a ×10 microscope objective was used to measure solid lysozyme spectra while a 0.25-in. immersion probe was employed to measure lysozyme aqueous solution spectra. All aqueous solution spectra were obtained with the 0.25-in. immersion probe, while the vessel was covered with aluminum foil to prevent light from external sources.

Experimental Design and Statistical Analysis

An experimental design was followed to obtain the maximum amount of relevant information while performing a minimum number of experiments. A number of experiments chosen through a D-optimal design were used to identify the significant factors. The Raman scattering of lysozyme solutions was considered as a function of three factors selected on the basis of previous studies: precipitating agent (NaCl), temperature, and time [14]. The optimi-

zation based on the D-optimal design was used to obtain the best conditions for the crystallization of the lysozyme protein. This approach facilitated a first stage of the optimization that consisted in a study of the variables that affect the system. The D-optimal design included 18 experimental runs with one central point. The levels of control are listed in Table 1.

The second step of the optimization was the study of the relationship between selected experimental factors and the several spectral bands where Raman scattering changes according to the different factor levels. The selected spectral bands were: 2,940, 760, 750, 155, and the 760/750 cm^{-1} ratio. The D-optimal design generates a polynomial mathematical model, an equation that relates the scattering of the lysozyme solutions measured at each individual Raman shift to the significant factors obtained in the previous crystallization experiment [19]. The model obtained is based on the following equation:

$$\hat{y} = \beta_0 + \sum \beta_0 x_i + \sum \beta_{ij} x_i x_j + \sum \beta_{ii} x_i^2 + \varepsilon \quad (1)$$

where $\hat{y}$ is the predicted response, β_i is the adjusting coefficient, and x_i, x_j are the factors studied, and ε is the residual error or bias [19]. This model allows the direct evaluation of the variables considered, and also the first-order interactions and quadratic terms. Randomization was used in order to obtain a random distribution of unknown systematic errors. The R^2 and Q^2 parameters (Eqs. 2 and 5) were used to evaluate the goodness of fit for each model.

$$R^2 = \frac{(\mathrm{SS} - \mathrm{SS_{RES}})}{\mathrm{SS}} \quad (2)$$

$$\mathrm{SS} = \sum_i (y_i - \bar{y})^2 \quad (3)$$

$$\mathrm{SS_{RES}} = \sum_i (y_i - \hat{y}_i)^2 \quad (4)$$

$$Q^2 = 1 - \frac{\mathrm{PRESS}}{\mathrm{SS}} \quad (5)$$

$$\mathrm{PRESS} = \sum_i \frac{(y_i - \hat{y}_i)^2}{(1 - h_i)^2} \quad (6)$$

Table 1 Factors in the experimental design

Factors	Units	Levels
Precipitant agent (NaCl)	% (*w*/*w*)	0, 5, 7, 9
Temperature	°C	15, 20, 25, 30, 35, 40, 45
Time	Hour	0, 3, 6, 9

Where y and $\hat{y}$ are the reference and predicted responses, respectively, and h_i is the ith diagonal element of the Hat matrix: $\mathbf{X(X'X)^{-1}X'}$. $\mathbf{X}$ is the factor matrix of the design. The Modde v8 software (Umetrics, Kinnelon, NJ, USA) was used for the calculations that supported the experimental design.

Lysozyme Protein Crystallization Studies

Batch crystallization was performed by mixing 500 μL of the precipitating agent and 500 μL of 100 mg/mL stock lysozyme solution in a scintillation vial to achieve supersaturation. Precipitating agent solutions ranging from 0% to 9% (*w*/*w*) NaCl were prepared in the acetate buffer. All experiments were performed in 0.1 M acetate buffer at pH 4.5. The protein solutions and the precipitating agent were mixed at ambient temperature, and then quickly placed in a Thermo Neslab water circulating bath connected to a 1,000-mL jacketed glass vessel used to control temperature of the lysozyme aqueous solution. All process measurements were obtained with a 0.25-in. immersion probe placed vertically inside the crystallization solution, while the vessel was covered with aluminum foil to prevent light from external sources. Raman spectra of protein batch crystallization solutions were acquired at different temperatures ranging from 15°C to 45°C throughout 9 h per each sample. The Raman spectra were collected 10 min after reaching each new temperature of the water bath. This waiting period was necessary to achieve thermal equilibrium.

Polarized Light Microscopy

An Olympus (Center Valley, PA, USA) CX31 polarized light microscope (PLM) was used as a supporting technique in this study. The solids were observed after the final stages of the batch crystallization experiment and mounted on a glass slide with a cover glass. A ×20 magnification was used to evaluate the crystal habit, crystal size distribution, and morphology of the crystals. PLM was also used to determine whether the solids obtained were amorphous or crystalline.

Results and Discussion

Lysozyme is a protein that contains 129 amino acids, and its three dimensional structure is stabilized by four disulfide bonds formed by four consecutive cysteines (Cys^6–Cys^{30}, Cys^{64}–Cys^{76}, Cys^{80}–Cys^{94}, Cys^{115}–Cys^{127}) [18]. Figure 1 shows the different lysozyme spectral bands that increase as the concentration is varied from 0–90 mg/mL in aqueous acetate buffer solutions. Figure 1 shows that Raman spectra of the lysozyme solutions also include bands related to the

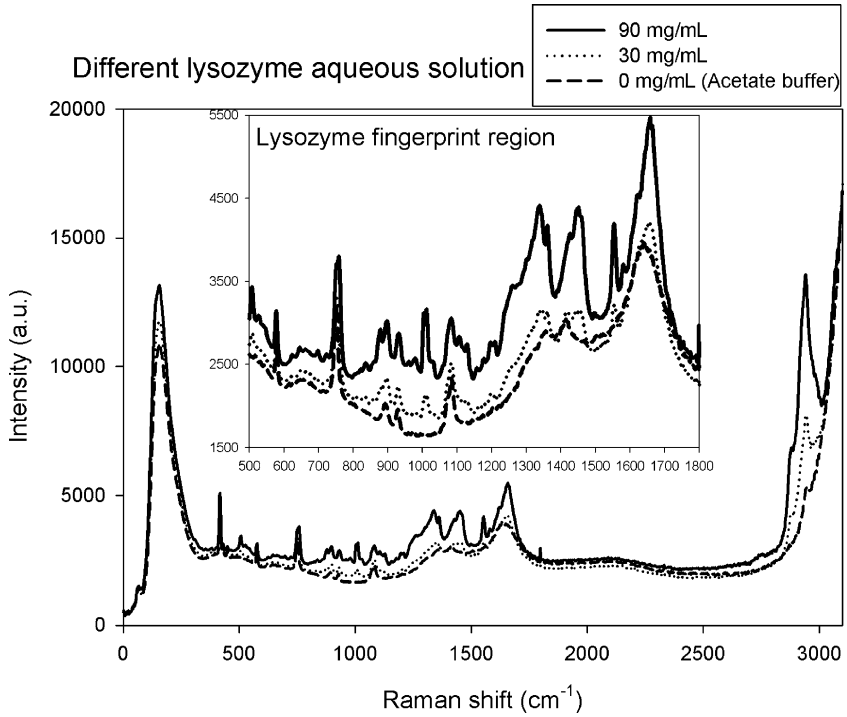

Fig. 1 Raman spectra for buffer and lysozyme aqueous solutions

acetate buffer. The acetate buffer generates bands at 1,660 and 3,300 cm^{-1} that correspond to the O–H bending and O–H stretching modes, respectively [20]. The buffer spectra also show a C–H stretching band near 2,940 cm^{-1}; however, the significant spectral changes observed in Fig. 1 as the protein concentration is varied permit monitoring the protein in solution in spite of the buffer spectral contribution. In addition to these bands, two additional weak bands can be observed at 420 and 750 cm^{-1}. Hédoux studied the Raman scattering of dried lysozyme with a band centered at 155 cm^{-1} that widened as the protein was hydrated [21]. The 155 cm^{-1} band has been associated with intermolecular O–H interactions in the hydrogen bond network of water and lysozyme [21, 22]. The acetate buffer also shows Raman scattering in this region, as evidenced in Fig. 1 where this band widened between 90 and 300 cm^{-1} becoming stronger in intensity as the lysozyme concentration increased.

The addition of precipitating agent to 100 mg/mL lysozyme solutions was followed by careful observation of the changes in the Raman spectra. Figure 2 shows spectra obtained 9 h after adding the precipitating agent solution to a 100-mg/mL lysozyme solution. The intensity of the lysozyme Raman spectral bands decreases with an increase of the sodium chloride concentration. The strong band at 2,940 cm^{-1}, that is associated with the $-CH_3$ asymmetric stretching vibration modes of the aliphatic residues, decreases as the NaCl concentration increases [23]. Figure 2 shows the decrease in the 760 cm^{-1} and increase in the 750 cm^{-1} spectral band corresponding to aromatic ring vibrational mode of tryptophan and the C–H rocking vibration of the acetate, respectively [24]. The S–S stretching vibration mode is observed at 520 cm^{-1} in the solid state, and 510 cm^{-1} in solution, but this is a weak band and was not used to monitor the protein in solution [23, 24]. Figure 2 also shows a reduction in the intensity of the155 cm^{-1} band.

The reduction of the lysozyme Raman scattering is due to a decrease in protein solution concentration when compared to the initial lysozyme protein concentration. These changes are attributed to the formation of lysozyme aggregates in the early stage of the protein crystallization process. After adding sodium chloride, colloidal particles can be observed in the lysozyme aqueous solution at low temperature, thus, indicating that supersaturation of the lysozyme solution was achieved. Supersaturation of the lysozyme aqueous solution occurs because the solubility of the lysozyme decreased with an increase of sodium chloride at low temperature. Wilson showed that the lysozyme forms monomers and dimers in sodium chloride aqueous solution, and these forms coexist within the lysozyme solubility limit [15]. The spectral changes observed as the sodium chloride was added indicated that the Raman spectrum was sensitive to protein nucleation. Thus, a study was performed to determine which of the Raman bands best reflected the changes in the solution.

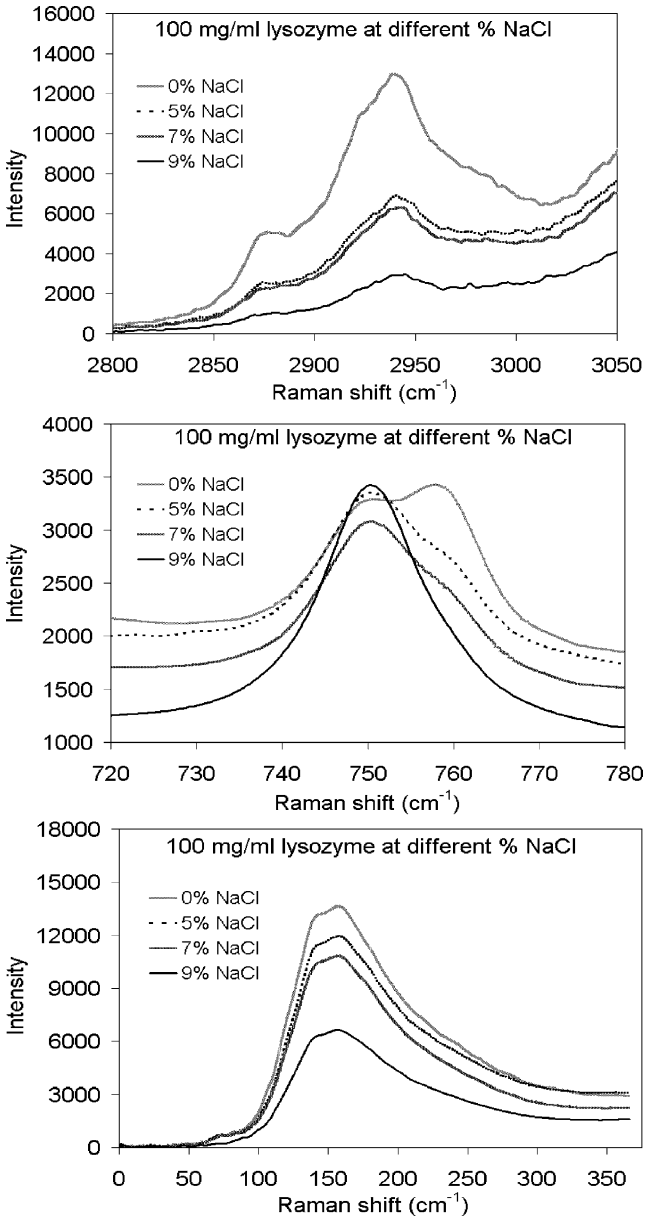

Fig. 2 Changes in Raman scattering that occur on addition of NaCl. Highest concentration of precipitating agent corresponds to bottom spectrum

Eighteen experiments were evaluated to determine the Raman scattering that best reflected the changes in solution. The study included three factors (percent of sodium chloride, temperature, and time of crystallization), and several levels as shown in Table 1. The factors selected for this study were the temperature ranging from 15°C to 45°C, sodium chloride ranging from 0% to 9% (*w*/*w*) and the time of crystallization that extended up to 9 h. Table 2 shows the design matrix for the experimental design and the relative intensities of the 2,940-, 760-, 750-, and 155-cm^{-1} spectral bands and the ratio between the 760/750 cm^{-1} bands evaluated in this study. Several other bands were also evaluated to develop the model relating the experimental factors studied to changes in the Raman spectra. However, the best correlations were obtained with the bands described in Table 2.

An initial polynomial model was calculated for each spectral response considering the three factors studied, their interactions, and the quadratic terms to evaluate the response that provides the highest correlation. Figure 3 presents the summary plots that describe the lysozyme crystallization regression model. The R^2 and Q^2 represent the fraction of variation of the response explained and predicted by the model, respectively, where a value of 1 is the maximum possible value. The band at 2,940 cm^{-1} and the ratio between the 760/750 cm^{-1} bands presented the highest correlation between these two values. The R^2 and Q^2 values for the 2,940 cm^{-1} band were 0.975 and 0.892, respectively. These results indicate that the model has small prediction errors and hence a good predictive ability. The ratio between the 760/750 cm^{-1} bands also present a good predictive model with values of 0.950 and 0.748. By contrast, the 155 and 760 cm^{-1} bands present a high percent of R^2 and a moderate model validity indicating that the lysozyme crystallization model contains a large prediction error value. Finally, the 750 cm^{-1} band yielded a poor model fitting and, therefore, a poor model validity. These results suggest that the 2,940-cm^{-1} band and the 760:750 ratio can be used to evaluate the variation of the lysozyme crystallization process as a function of the three factors (percent of sodium chloride, temperature, and time of crystallization) selected.

The proposed regression model was established with the 2,940 cm^{-1} band that presented the highest correlations. The obtained equation considered the three factors studied, their interactions, and the quadratic terms. The main factor affecting the relative intensity of the lysozyme was the sodium chloride concentration and its quadratic term, as shown in Fig. 4. Higher NaCl concentrations lead to lower Raman intensities, and an increase in the protein crystallization can be observed. The second factor affecting the lysozyme crystallization is the temperature and also its quadratic term. At high temperatures, the protein solubility increases and, hence, the relative intensity of the lysozyme Raman scattering. The factor time, its interactions, and quadratic term had a poor correlation with the relative intensity of the lysozyme bands. For this reason, the factor time and its interactions were excluded from the evaluation, obtaining the equation coefficients presented in Fig. 5. All the factors included in Fig. 5 are significant, and the polynomial regression presents a correlation coefficient (R^2 and Q^2) of 0.964 and 0.928, respectively. Figure 5 also shows a negative correlation between NaCl concentration

Table 2 Raman intensities obtained for solutions prepared following experimental design for the lysozyme protein crystallization study

Runs	Percent NaCl	Temperature (°C)	Time (h)	Raman intensity				
				760 cm^{-1}	750 cm^{-1}	2,940 cm^{-1}	155 cm^{-1}	Abs_{760}/Abs_{750}
1	0	15	0	3,292	3,161	12,061	11,895	1.041
2	7	15	0	1,794	3,170	2,928	3,531	0.566
3	9	20	0	1,441	2,011	3,316	4,907	0.717
4	5	35	0	3,402	3,775	8,718	14,326	0.901
5	0	45	0	3,223	3,171	11,451	12,412	1.016
6	9	45	0	2,925	3,586	7,069	11,738	0.816
7	9	15	3	1,928	3,251	3,246	4,871	0.593
8	0	25	3	4,069	3,986	14,106	14,333	1.021
9	5	45	3	2,860	3,283	7,149	13,004	0.871
10	5	20	6	2,159	2,639	5,040	7,732	0.818
11	9	35	6	2,770	3,170	7,586	12,247	0.874
12	7	45	6	2,544	3,347	5,856	10,442	0.760
13	0	15	9	3,298	3,191	12,038	11,908	1.034
14	9	15	9	1,899	3,252	3,329	4,890	0.584
15	7	25	9	2,833	3,571	7,183	11,204	0.793
16	0	40	9	3,434	3,370	11,407	12,549	1.019
17	0	45	9	3,316	3,222	11,132	12,430	1.029
18	9	45	9	2,554	3,190	6,368	10,274	0.801

and the Raman signal, and positive correlation between temperature and Raman signal resulting from the higher protein solubility.

The lysozyme crystallization can also be evaluated using contour plot maps. The contour plot maps can be used to track changes in the solubility of the lysozyme as the NaCl and temperature are varied. Similarly, an interpretation of the appropriate conditions for the lysozyme crystallization process can be established, and new situations can be predicted. The proposed model describes the correlation between the factors selected and the response of the relative intensity of the lysozyme for the 2,940-cm^{-1} band. The three-dimensional contour plots map can be observed in Fig. 6. Figure 6a shows that the larger NaCl concentration facilitates protein crystallization (decreasing the Raman scattering), but this effect depends on the temperature of the solution (Fig. 6b). The lower temperatures induce higher crystallization. The morphology of the crystals obtained

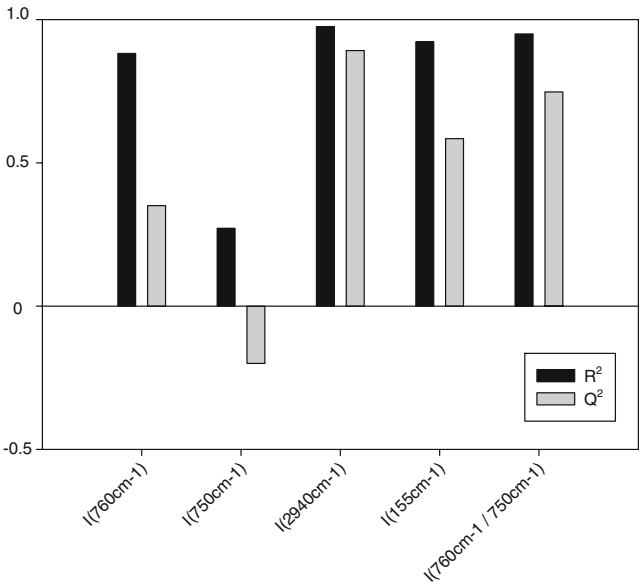

Fig. 3 Summary plot of the correlations at different lysozyme protein Raman bands

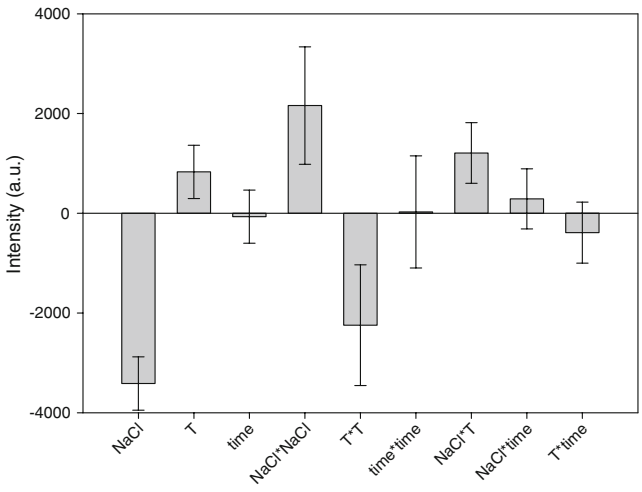

Fig. 4 Scaled and centered equation coefficients for I (2,940 cm^{-1}) including time factor (error bar means confidence interval α=0.05, R^2=0.975, Q^2=0.892)

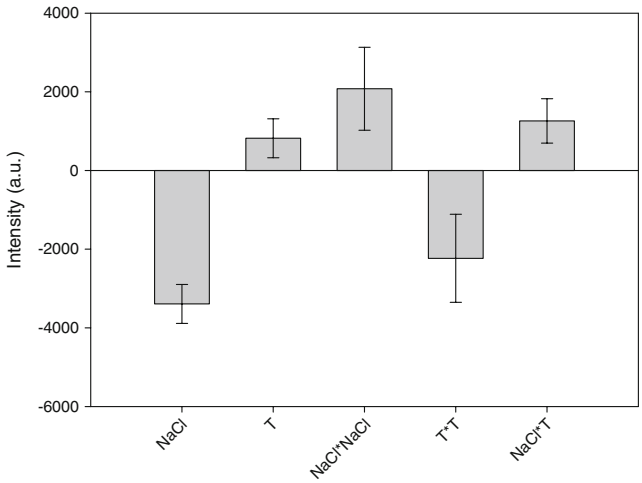

Fig. 5 Scaled and centered equation coefficients for I (2,940 cm^{-1}) *not* including time factor (error bar means confidence interval α=0.05, R^2=0.964, Q^2=0.928)

depends on the different experimental conditions of temperature and NaCl concentration represented on the surface plot. The different crystals were analyzed by polarized light microscopy in order to correlate the crystallization conditions with the morphology of the crystals.

Figure 7 shows significant differences in the particle size and morphology of the crystals obtained at the various conditions studied. The top row shows that few but large crystals are obtained at 45°C and 5% NaCl, and the number of crystals increases as the NaCl is increased (left to right). Figure 7 also shows that a higher number of crystals was obtained as the temperature is reduced (top to bottom). At low temperature and high 9% NaCl concentration (photograph m), crystal growth was rapid and uncontrolled yielding amorphous solids. All the other conditions yielded crystals.

The 3D response surface plot, for the 2,940 cm^{-1} band, may be used to visualize the different conditions evaluated in this study and is especially valuable when combined with polarized light microscopy as shown in Fig. 7. When the NaCl concentration is low, Raman scattering remains high, indicating that lysozyme is dissolved, and crystals will not be observed. However, as the NaCl concentration increases, Raman scattering decreases. The decrease in the Raman scattering at 2,940 cm^{-1} is quite pronounced at temperatures below 25°C. Low temperature and high NaCl promote a rapid crystal nucleation of amorphous particles that corresponds to Fig. 7m. The crystals observed in photographs a–c in Fig. 7 correspond to the high temperature section of the 3D response surface plot. Certainly, the conditions of 35–40°C and 5–9% NaCl can be defined as a meta-stable zone, where the crystal growth is promoted. The surface shows that above 30°C, increases in NaCl result in a less pronounced reduction of the Raman signal. Therefore, if large crystals are desired the response surface indicates that temperatures above 35°C are required. On the other hand, if amorphous, more soluble solids are needed, then high NaCl and temperatures below 20°C would be recommended. The surface response plots constitute a powerful tool for the design of a crystallization process.

Figure 7g,h, and i present the lysozyme crystal growth at 20°C and different NaCl concentrations. The number of crystals observed depends on the sodium chloride concentration, with only a few lysozyme crystals observed at 5% NaCl, and the greatest number observed at 9% NaCl. Similar results can be observed at 25°C in Fig. 7d–f. Finally, when the temperature increases to 45°C (Fig. 7a–c fewer crystals were observed even with a high NaCl concentration. This study suggests that the morphology and the crystal size distribution of the lysozyme depend on the temperature and NaCl concentration.

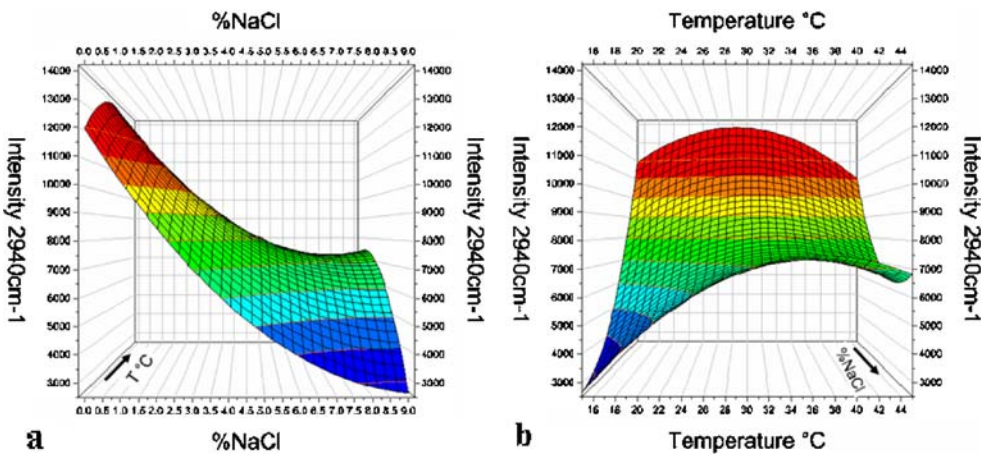

Fig. 6 Surface response plots for 2,940 cm^{-1} band vs **a** NaCl concentration in the *x*-axis and temperature increasing from front to back in *z*-axis and **b** temperature in *x*-axis and NaCl concentration increasing from back to front

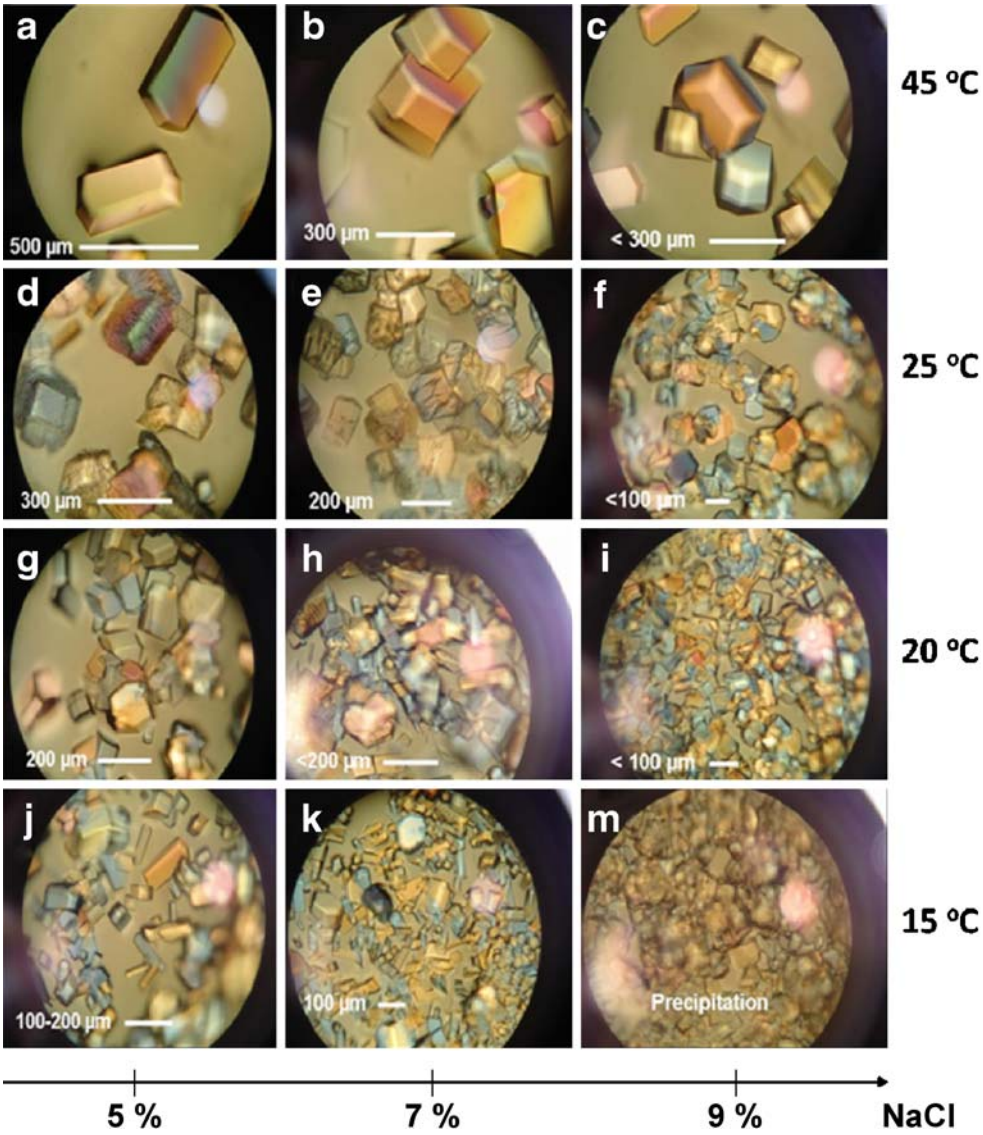

Fig. 7 Lysozyme protein crystal growth from left to right: 5%, 7% and 9% percent of sodium chloride at different temperatures from top to bottom: 45°C, 25°C, 20°C, 15°C, respectively. The letter m has been used instead of "l" to avoid confusion with the number 1. **a** 500 µm, **b** 300 µm, **c** <300 µm, **d** 300 µm, **e** 200 µm, **f** <100 µm, **g** 200 µm, **h** <200 µm, **i** <100 µm, **j** 100–200 µm, **k** 100 µm, **m** Precipitation

The surface plot obtained with the polynomial equation (Fig. 6) can be related with the effect of the crystallization conditions on the morphology of the obtained crystals. The crystals shown in Fig. 7m (small and irregular) are those obtained on the conditions represented in the surface plot region colored in blue (Fig. 6), whereas the surface plot plateau colored in light green is related with the crystals of Fig. 7a,b (large and well defined crystals).

The authors recognize that additional research efforts would still be necessary to adapt the method to large-scale manufacturing. For example, the study did not take into consideration the possible effects of agitation, where Raman measurements could include scattering from both dissolved and solid forms. This limitation could be overcome by determining the concentration of dissolved and solid forms using a second method as shown in a previous study where the benefits of Raman spectroscopy were demonstrated even when the vessel was agitated [5].

Conclusion

Raman scattering may be used to design and monitor a crystallization process. The approach followed in this study may be performed with a single protein solution allowing the design of the crystallization process before large amounts of the protein are available. The design provides significant process knowledge demonstrating that NaCl concentration and temperature are the critical process parameters. Raman scattering was effective in monitoring the progress of the protein crystallization and could be the basis of future process control efforts.

Acknowledgements The authors thank INDUNIV (Puerto Rico Industry, Government, and University Research Consortium), and the NSF Engineering Research Center for Structured Organic Particulate Systems (ERC-SOPS) for funding this study. A special gratitude is also extended to Dr. Naír Rodríguez Hornedo from the Department of Pharmaceutics at the University of Michigan for

stimulating discussions on nucleation and crystallization, and Vladimir Vélez from Lilly del Caribe for suggesting this research project.

References

1. FDA. PAT—a framework for innovative manufacturing and quality assurance; 2004.
2. Romañach RJ. Is PAT the beginning of a revolution in pharmaceutical manufacturing?—a personal interpretation of the PAT initiative. J Proc Anal Tech 2004;1(1):10–2.
3. Romañach RJ. Research initiatives to support science-based pharmaceutical manufacturing. Pharm Tech Europe 2007;19(10):47–51.
4. Zhou GX, Crocker L, Xu J, Tabora J, Ge Z. In line measurement of a drug substance via near infrared spectroscopy to ensure a robust crystallization process. J Pharm Sci 2006;95:2337–47.
5. Hu Y, Liang J, Myerson A, Taylor LS. Crystallization monitoring by Raman spectroscopy: simultaneous measurement of desupersaturation profile and polymorphic form in flufenamic acid systems. Ind Eng Chem Res 2005;44:1233–40.
6. Yu LX, Lionberger RA, Raw AS, D'Costa R, Wu H, Hussain AS. Applications of process analytical technology to crystallization processes. Adv Drug Delivery Rev 2004;56:349–69.
7. Févotte G. New perspectives for the on-line monitoring of pharmaceutical crystallization processes using in situ infrared spectroscopy. Int J Pharm 2002;241:263–78.
8. Tamagawa RS, Miranda EA, Berglund KA. Raman spectroscopy monitoring and control of aprotinin supersaturation in hanging-drop crystallization. J Cryst Growth 2002;2:263–7.
9. Tamagawa RS, Miranda EA, Berglund KA. Simultaneous monitoring of protein and $(NH_4)_2SO_4$ concentrations in aprotinin hanging-drop crystallization using Raman spectroscopy. J Cryst Growth 2002;2:511–4.
10. Schwartz A, Berglund KA. Comparison of supersaturation profiles employed on lysozyme crystallization from a hanging drop. J Cryst Growth 2001;1:81–5.
11. Schwartz A, Berglund KA. In situ monitoring and control of lysozyme concentration during crystallization in a hanging drop. J Cryst Growth 2000;210:753–60.
12. Schwartz A, Berglund KA. The use of Raman spectroscopy for in situ monitoring of lysozyme concentration during crystallization in a hanging drop. J Cryst Growth 1999;203:599–603.
13. International conference on harmonisation of technical requirements for registration of pharmaceuticals for human use, ICH Harmonised Tripartite Guideline, Pharmaceutical Development Q8, Step 4, 10-November-2005.
14. Gorti S, Forsythe EL, Pusey ML. Growth rates and energetics of (101) face lysozyme crystal growth. Cryst Growth Des 2005;5:473–82.
15. Wilson LJ, Kim YW, Baird JK. Lysozyme self-association in aqueous solution NaCl at pH 4.0 and 20°C. Cryst Growth Des 2002;1:41–3.
16. Prater BD, Truller SC, Wilson LJ. Simplex optimization of protein crystallization conditions. J Cryst Growth 1999;196:674–84.
17. Knezic D, Zaccaro J, Myerson AS. Thermodynamic properties of supersaturated protein solutions. Cryst Growth Des 2004;4:199–208.
18. Chang JY, Li L. The unfolding mechanism and disulfide structures of denatured lysozyme. FEBS Lett 2001;487:73–8.
19. Massart DL, Vandeginste BGM, Buydens LMC, De Johg S, Lewi PJ, Smeyers-Verbeke J. Handbook of chemometrics and qualimetrics part A. 1st ed. Amsterdam: Elsevier; 1997.
20. Lin-Vien D, Colthup NB, Fateley WG, Grasselli JG. The handbook of infrared and Raman characteristic frequencies of organic molecules. 1st ed. San Diego: Academic Press; 1991.
21. Hedoux A, Affouard F, Descamps M. Microscopic description of protein thermostabilization mechanism with disaccharides from Raman spectroscopy investigation. J Phys Condens Matter 2007;19:205142–9.
22. Giraud G, Karolin J, Wynne K. Low frequency modes of peptides and globular proteins in solution observed by ultrafast OHD-RIKES spectroscopy. Biophys J 2003;85:1903–13.
23. Howell NK, Arteaga G, Nakai S, Li-Chan ECY. Raman spectral analysis in the C–H stretching region of proteins and amino acids for investigation of hydrophobic interactions. J Agric Food Chem 1999;47:924–33.
24. Howell N, Chan EL. Elucidation of interactions of lysozyme with whey proteins by Raman spectroscopy. Int J Food Tech 1996;31:439–51.